European Journal of Medicinal Chemistry Reports 13 (2025) 100248

Contents lists available at ScienceDirect

European Journal of Medicinal Chemistry Reports

journal homepage: www.editorialmanager.com/ejmcr/default.aspx

Synthesis, evaluation of the biological activity against *Trypanosoma cruzi* and *Leishmania donovani*. Preliminary *in silico* ADMET studies of 5-nitroimidazole derivatives

Miguel A. Rodríguez [a], Ali Mijoba [a,b], Nereida J. Parra-Giménez [b,***], Zuleyma Blanco [a], Katiuska Chávez [c], Alirica I. Suárez [c], Esteban Fernandez-Moreira [d], Hegira Ramírez [e,**], Jaime E. Charris [a,*]

[a] *Laboratorio de Síntesis Orgánica, Facultad de Farmacia, Universidad Central de Venezuela, Apartado 47206, Los Chaguaramos, 1041-A, Caracas, Venezuela*
[b] *Laboratorio de Fisiología de Parásitos. Centro de Biofísica y Bioquímica, Instituto Venezolano de Investigaciones Científicas (IVIC), Altos de Pipe, Caracas, Venezuela*
[c] *Laboratorio de Productos Naturales, Facultad de Farmacia, Universidad Central de Venezuela, Los Chaguaramos, 1041-A, Caracas, Venezuela*
[d] *Escuela de Medicina, Universidad Espíritu Santo, Samborondón, 092301, Ecuador*
[e] *Universidad ECOTEC, Km. 13.5 Vía Samborondón, Samborondón, Guayas, 092302, Ecuador*

ARTICLE INFO

Keywords:
Chagas disease
Leishmania donovani
Totoxicity assay
5-Nitroimidazole
Hybridation

ABSTRACT

The synthesis and evaluation of the biological activity of a series of 5-nitroimidazole hybrids is described. The structures of the synthesized hybrids were confirmed by spectral analysis FT-IR, ^{1}H NMR, ^{13}C NMR, MS, and by Elemental Analysis. The toxicity (ADME/Tox) assessment study were carried out to predict the molecular properties associated with pharmacokinetic aspects of novel compounds. The trypanocidal and leishmanicidal activities of all synthesized hybrids were evaluated, compounds **7a** and **8b** were active against the epimastigote form of *T. cruzi*. Compound **10b** showed marginal activity against the promastigote form of *L. donovani*. Sulfonyl derivative **8b** was the most promising compound with IC_{50}: 9.58 ± 2.02 μM and with a selectivity index (SI) greater than 31.31, that justifies the description as a promising hit for further study as a possible antichagasic agent.

1. Introduction

Millions of people around the world are affected by trypanosomatids, parasites that cause serious illnesses in those who suffer from them. In The Americas, these kinetoplastids cause Chagas disease (CD) (*Trypanosoma cruzi*) and Leishmaniasis is caused by over 20 *Leishmania* species. These Neglected tropical diseases (NTDs) limit human potential and are especially harmful to vulnerable populations [1].

Both *T. cruzi* and *Leishmania* share the characteristic of being heteroxenic parasites, developing their life cycles between an invertebrate vector and a vertebrate host (Fig. 1). Throughout their complex life cycles, they develop morphological stages whose susceptibility to drugs varies depending on their location in the host. Epimastigotes and metacyclic trypomastigotes are found in the intestinal tract of the Triatominae vector of *T. cruzi* (Fig. 1a), while procyclic and metacyclic promastigotes are found in the midgut of the Phlebotominae vector of the *Leishmania* genus (Fig. 1b) [2,3]. Furthermore, both parasites progress to intracellular amastigote forms in the vertebrate host, which in *T. cruzi* give rise to blood trypomastigote forms.

CD or American trypanosomiasis transmitted by blood-sucking triatomine bugs, is endemic in 21 countries, affects an estimated 8–10 million people worldwide, 30 % of whom will develop chronic Chagas cardiac disease, and as a consequence will cause approximately 14000 deaths each year [4]. However, and despite these alarming numbers, there are only two drugs available for treating Chagas disease: benznidazole (Bzn) and nifurtimox (Nfx) (Fig. 2). Although these drugs are effective in the initial phase, they are limited in their effectiveness for chronic infections, and both drugs are restricted because of their toxic effects [5,6].

Fexinidazole (Fx) represents an important advance in CD drug

* Corresponding author.
** Corresponding author.
*** Corresponding author.
E-mail addresses: bionereida@gmail.com (N.J. Parra-Giménez), hegiraipc@gmail.com (H. Ramírez), jaime.charris@ucv.ve (J.E. Charris).

https://doi.org/10.1016/j.ejmcr.2025.100248
Received 3 December 2024; Received in revised form 14 January 2025; Accepted 23 January 2025
Available online 25 January 2025

discovery. In October 2017, a new phase II study was initiated with Fx using shorter, lower-dose treatment regimens. The study was completed in 2019 and the results were available in 2022. Fx effectively eliminated parasitemia in all patients, but it was discontinued due to safety concerns related to adverse events (Fig. 2) [7,8].

Leishmaniasis, caused by different species of the genus *Leishmania* and transmitted by sand flies, currently affects around 12 million people globally and it is spreading rapidly with 0.7–1 million new cases and around 30000 deaths annually [9]. The disease comprises three major syndromes: cutaneous, mucocutaneous and visceral leishmaniasis. The visceral form is known to cause a 95 % death rate among the poorest people in the world. The main chemotherapy for the treatment of leishmaniasis has been based for over 60 years on the use of pentavalent antimonial drugs being meglumine antimoniate (Glucantime™) or sodium stibogluconate (Pentostam™) the first-choice drugs, which are highly toxic. Amphotericin B (Aph-B) and miltefosine (Mtf) are both second-line drugs that are used when antimonial drugs fail to work for patients (Fig. 3). However, use in endemic areas is limited due to their toxicity, significant drawbacks like the length of treatment, complicated route of administration, the rise of drug resistance, and costs [10–12].

The challenges of chemotherapy in treating CD and leishmaniasis have prevented the preclinical phase from examining new molecules, this has encouraged various research groups to conduct diverse studies that seek to repurpose and hybridize drugs for other diseases, and their adaptability to treat CD and leishmaniasis [13–17]. In our quest for new chemical entities that have leishmanial and antitrypanosomal properties, we wanted to examine whether metronidazole (Mtz) hybridized with certain pharmacophores, could be a potential candidate for treatment of these diseases. The first 5-nitroimidazole drug introduced to human therapy, MTZ, was used to treat trichomoniasis, followed by its use to treat infections caused by a range of anaerobic and microaerophilic bacteria, including *Giardia lambia*, *Tricomonas vaginalis*, *Entamoeba histolitica* and *blastocystis sp* protozoa including *C. difficile*, for which it is still prescribed today despite a range of adverse effects [18]. However, Mtz has not shown effectiveness when assessed against these two parasites [19]. Mtz behaves as a prodrug, it is bioreduced by type I nitroreductases in anaerobic or microaerophilic intracellular environments, resulting in radical nitro anions that are harmful to protozoa [20,21]. A chemical structure with the core of the 5-nitroimidazole and pharmacophoric groups such as esters or amides could allow us to design new hybrid molecules with a biological potential against the parasites that cause pathologies such as leishmaniasis and CD. In the literature, there are reports of Mtz-hybrids with different groups of pharmacophores with promising results against these trypanosomatids [22–24].

Based on our own experiences, in this work we report the synthesis of hybrid structures formed by the nucleus of Mtz with ester and amide groups, where we are using a fragment of mercaptoacetic acid or mercaptoethanol as a bridge group, a strategy widely used by our group to generate bioactive molecules [19,25–27]. In-silico profiling of absorption, distribution, metabolism, excretion, and toxicity (ADME/Tox) was also performed to predict the molecular properties associated with pharmacokinetic aspects of novel compounds.

2. Results and discussion

2.1. Chemistry

The sulfanyl and sulfonyl-tethered functionalized benzoate derivatives featuring a 5-nitroimidazole moiety **7a-d** and **8a-c**, respectively, were prepared by previously described methods [25]. Using metronidazole™ **1** as starting material, compounds **10a-h** were prepared as shown in Scheme 1. The primary alcohol of **1** was replaced by a chlorine atom following known procedures upon reaction with thionyl chloride, **1** was converted into the corresponding hydrochloride salt, which was then treated with water and Et_3N until pH 11, to obtain the 1-(2-Chloroethyl)-2-methyl-5-nitroimidazole **2** with a yield of 96 % [19,25]. Treatment of **2**, using sodium iodide in refluxing anhydrous acetone, gave the iodinated compound **3** in 96 % yield [19,25,28]. Next, the compounds **5** was prepared from derivative **3** by iodine nucleophilic substitution in the aliphatic portion using methyl thioglycolate in 83 % yield [19]. Compound **6** was obtained from **5** through modified experimental protocol using LiOH in a mixture of methanol:water 1:1 at room temperature (rt) with an even better yield in 97 %. Compounds **10a-h** were synthesized by a modified version of the Steglich esterification reaction at rt, between acid **6** with aniline respectives **9a-h**, in the presence of EDCI and DMAP in CH_2Cl_2 [29]. The title compounds were isolated in good-to-excellent yield (60–93 %) after purification by column chromatography (Scheme 1).

All these compounds were characterized based on their IR, NMR, mass spectra data, and their purity was ascertained by microanalysis. In general, the ^{1}H NMR spectrum showed a single signal ranging from δ H 7.9–8.2 ppm, which was assigned to the H-4 of the imidazole ring. The aromatic region of the ^{1}H NMR spectra featured signal patterns ranging from δ_H 6.6–7.4 ppm, characteristic of the substitution pattern of each

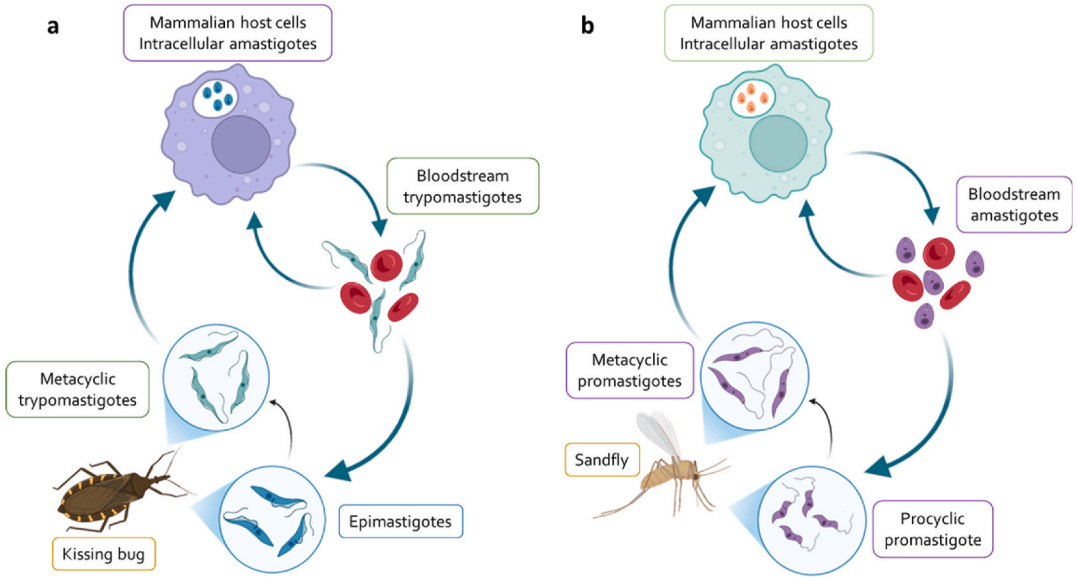

Fig. 1. The clinically relevant life-cycle stages of (a): *T. cruzi* and (b): *L. donovani*.

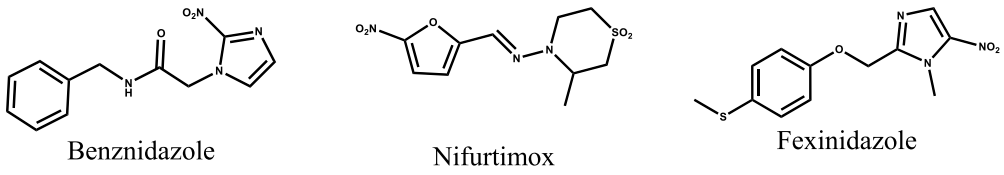

Fig. 2. Drugs in clinical use against Chagas disease.

aromatic ring. The aliphatic signals expected at upfield shifts were found from δ_H 3.0–4.5 ppm and confirmed by COSY experiments.

The ^{13}C NMR spectrum showed characteristic signals of the 5-nitroimidazole core, with one signal resonating at δ_C 140–165 ppm, attributed to C-5, as well as two signals observed in the δ_C 138–152 and 124–140 ppm regions, assigned to C-2 and C-4, respectively. For the carboxyl group, another characteristic signal was observed further downfield around δ_C 165–166 ppm. Aliphatic carbons were unequivocally confirmed by the DEPT 135° and HETCOR experiments (Supplementary information).

Using mass spectrometry, the formation of each final product was corroborated. The EI-MS of compounds **10a-h** exhibited the molecular ion peaks [M+] at *m/z* 350.10, 364.07, 348.10, 382.08, 427.90, and 410.14 for $C_{15}H_{18}N_4O_4S$, $C_{15}H_{16}N_4O_5S$, $C_{16}H_{20}N_4O_3S$, $C_{16}H_{19}ClN_4O_3S$, $C_{16}H_{19}BrN_4O_3S$, and $C_{17}H_{22}N_4O_6S$ molecular formulas, respectively, with the exception of compound **10e**, where the molecule undergoes a different fragmentation pattern with a peak at *m/z* 227.02 [$M^+ - C_8H_{10}N_3O_3S$] (Supplementary information). Peaks with 100 % abundance are attributed to the removal of the aromatic ring from [M^+].

The infrared (IR) spectra of the compounds show one characteristic intense stretching band between 1624 and 1683 cm^{-1}, for carbonyl of amide (R-CO-NHAr) present in all compounds (Supplementary information). The analytical data for compounds are summarized in the experimental section.

2.2. In silico analysis

Using *SwissADME*, drug-likeness descriptors were calculated according to Lipinski and Veber rules [30,31]. These descriptors and results indicating non-violation of Lipinski's rule of five could predict good absorption or permeation of each molecule, however, some exceptions to the "rule of five" for certain drug classes (e.g., vitamins, antifungals, antibiotics, and cardiac glycosides). Table 1 summarizes these results. With exception of compounds **8a**–**c**, in general, the compounds did not violate these rules according to these criteria.

In the BOILED-Egg illustration (Fig. 4), compounds **4**, **6**, **7d**, **10a-g**, and Mtz are predicted to demonstrate high gastrointestinal (GI) absorption; however, compounds **7a-c**, **8a-c**, and **10h** are predicted to demonstrate low GI absorption. The data predict that the reported compounds do not cross the blood-brain barrier. Except compounds **7a**, **7b**, **8a-c**, all compounds demonstrated a TPSA value < 140 $Å^2$, thus indicating their good oral bioavailability.

Fig. 5 summarizes the main ADME parameters in the radar representations for compounds Mtz, **7a**, **8a**, and **8b**, including properties such as lipophilicity, size, polarity, solubility, saturation, and flexibility. The colored zone represents the suitable physicochemical space for oral bioavailability, and the red bold line represents values of the calculated properties of the analyzed molecule. Mtz exhibited all of the properties characteristic of orally available drugs (see Fig. 5).

Motivated by the fact that the prediction values for GI absorption and bioavailability are low for the most active compounds *in vitro* **7a**, **8a**, and **8b**, we decided to determine the solubility in water for each of these compounds using the *SwissADME* program. Water solubility is a factor related to the route of administration, absorption, and pharmaceutical form. To predict water solubility, the program uses two topological methods: the ESOL (Estimated SOLubility) model [32] and a model incorporating the effect of topographical polar surface area [33], as well as a third predictor for solubility developed by SILICOS-IT. All predicted values are shown as decimal logarithms of the molar solubility in water (log S). Table 2 shows the calculated values for **7a**, **8a**, and **8b** derivatives (log S (ESOL) of −3.62, −2.91, and −2.91, respectively). An antiparasitic compound needs to reach the target to produce a positive effect. Thus, these values achieved by compounds **7a**, **8a**, and **8b** help us predict that the intraperitoneal route should be the best way to achieve a positive antiparasitic effect.

Several molecular descriptors complementing our *in silico* evaluation were calculated using *pkCSM-pharmacokinetics*, including the percentage of compounds **4**, **6**, **7a-d**, **8a-c**, and **10a-h** absorbed through the human intestine (%HIA). Appropriate values were considered in the range of 62.46 %–96.43 %. A molecule with an absorption of less than 30 % is

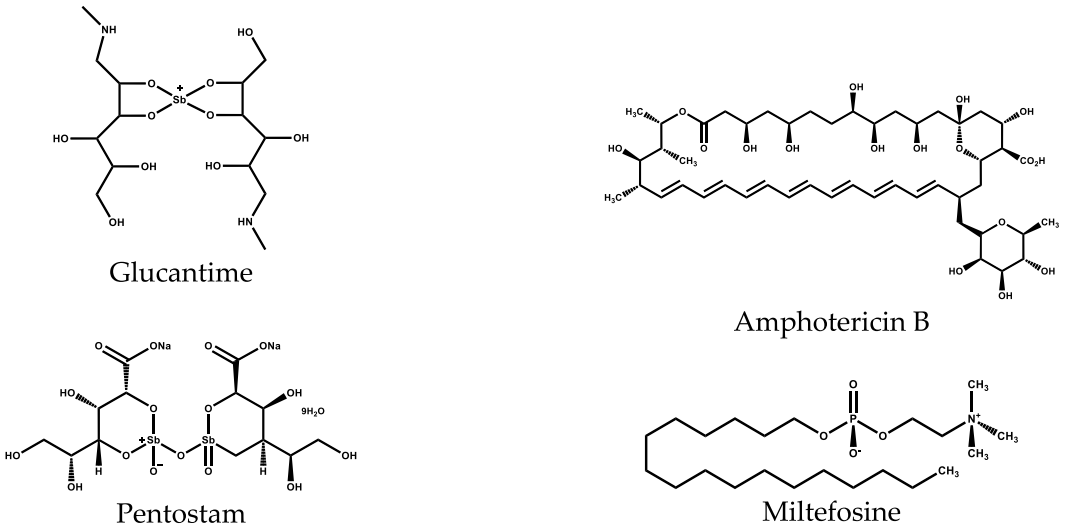

Fig. 3. Drugs in clinical use against leishmaniasis.

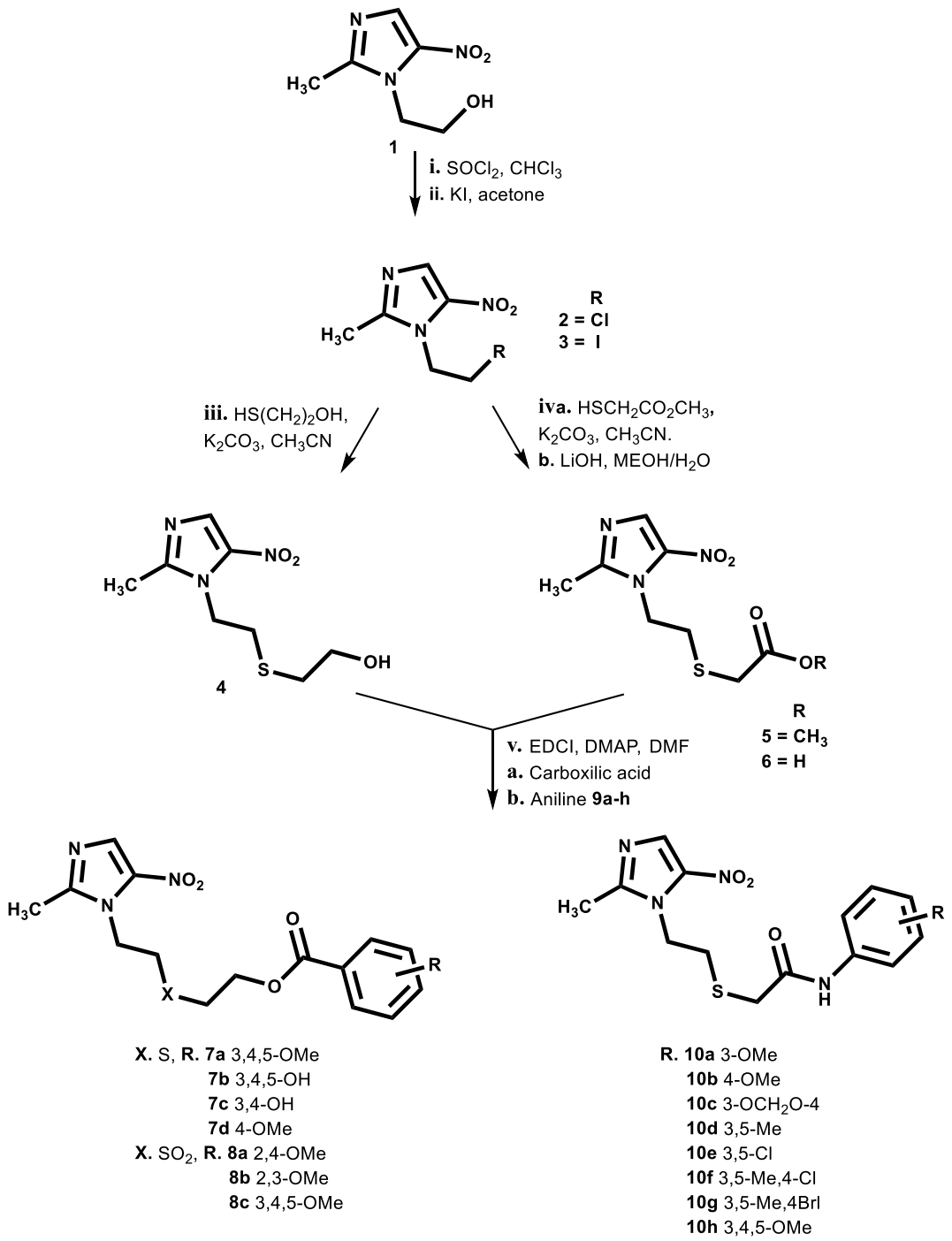

Scheme 1. Synthesis of the 2-{[2-(1H-imidazole-1-yl)ethyl]sulfanyl or sulfonyl}ethyl benzoate derivatives **7a-d**, **8a-c** and 2-{[2-(1H-imidazole-1-yl)ethyl]thio} acetamide derivatives **10a-h**.

considered poorly absorbed. In this study, the descriptors fraction unbound compound (FU) and total clearance (CLtot) were used to predict the distribution [34–36]. The effectiveness of a drug can be affected by the degree to which it binds to proteins within the blood, as increased binding reduces its ability to cross cell membranes efficiently. In this study, compounds **4**, **6**, **7a-d**, **8a-c**, **10a-h**, and Mtz had FU values between 0.222 and 0.658. The most active compounds **8a**, **b** had a value of about 50 % of the Mtz. Drug clearance occurs primarily as a combination of hepatic and renal clearance. It is related to bioavailability and is important for determining dosing rates to achieve steady-state concentration. The total clearance (CLtot) descriptor ranged from 0.344 to 0.819 ml/min/kg, for compounds **7a**, **8a**, and **8b** showing values of 0.686, 0.344, and 0.373 ml/min/kg, respectively.

The hepatotoxicity and oral toxicity LD_{50} values of compounds **4, 6, 7a-d, 8a-c, 10a-h,** and Mtz were predicted [34,37]. A compound is classed as hepatotoxic if it has at least one pathological or physiological liver event which is strongly associated with disrupted normal function of the liver. Predictions for the most active compounds **7a**, **8a**, and **8b** indicate that they are not hepatotoxic and with respect to LD_{50}, they are less lethal than Mtz.

The possibility that compounds **4**, **6**, **7a-d**, **8a-c**, **10a-h**, and Mtz are substrates or inhibitors of selected human transporters was analyzed.

Table 1
In silico evaluation of physicochemical properties of compounds **4, 6**, **7a–d**, **8a–c**, and **10a–h**.

No	Log P	MW	Hba	Hbd	Rotb	Viol	LogSw	%HIA	FU	CLtot	LD_{50}
4	0.46	231.27	4	1	6	0	−1.28	83.483	0.566	0.741	1.762
6	0.38	245.26	5	1	6	0	−1.53	62.462	0.584	0.399	1.696
7a	2.26	425.46	8	0	12	0	−3.62	81.12	0.293	0.686	2.378
7b	0.92	383.38	8	3	9	0	−2.91	70.947	0.386	0.664	2.229
7c	1.38	367.38	7	2	8	0	−3.11	80.396	0.373	0.711	1.941
7d	2.1	365.40	6	0	10	0	−3.40	91.238	0.222	0.742	2.278
8a	1.35	427.43	6	0	11	1	−2.91	90.634	0.385	0.344	2.381
8b	1.34	427.43	6	0	11	1	−2.91	93.676	0.385	0.373	2.442
8c	1.08	457.45	10	0	12	1	−2.62	85.364	0.366	0.408	2.455
10a	1.34	350.39	5	1	9	0	−2.90	89.045	0.288	0.666	2.433
10b	1.32	350.39	5	1	9	0	−2.90	86.121	0.315	0.701	2.406
10c	1.3	364.38	6	1	8	0	−3.08	96.434	0.272	0.813	1.738
10d	2.13	348.42	4	1	8	0	−3.43	91.272	0.261	0.670	1.802
10e	2.51	389.26	4	1	8	0	−4.02	88.355	0.251	0.470	1.865
10f	2.59	382.87	4	1	8	0	−4.03	91.267	0.253	0.741	1.825
10g	2.7	427.32	4	1	8	0	−4.34	91.200	0.250	0.819	1.829
10h	1.4	410.44	7	1	11	0	−3.20	80.210	0.376	0.669	2.306
Mtz	−0.1	171.15	4	1	3	0	−1	92.759	0.658	0.48	1.759

Log P, partition coefficient; MW, molecular weight; Hba, hydrogen bond acceptors; Hbd, hydrogen bond donors; Rotb, rotatable bonds; Viol, Lipinski's violations; LogSw: water solubility; HIA, human intestinal absorption; FU, fraction unbound; CLtot, total clearance; LD_{50}, oral rat acute toxicity; Mtz: Metronidazole.

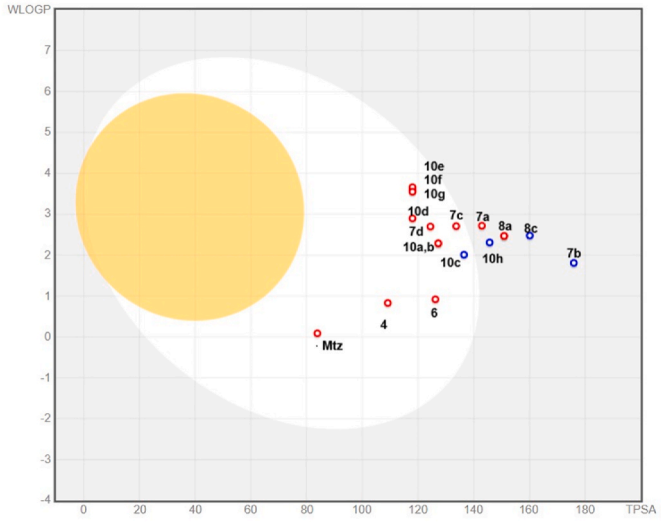

Fig. 4. BOILED-Egg compounds **4**, **6**, **7a-d**, **8a-c**, **10a-h**, and Mtz.

The targets can be P-glycoprotein, which is vital in cell distribution and excretion. The ADMET Predictor software *pkCSM-pharmacokinetics* revealed that all compounds are P-glycoprotein substrates. Concerning inhibitory action, the most actives compounds **7a**, **8a**, **8b**, and Mtz examined are inhibitors of P-glycoprotein I, however against P-glycoprotein II, only compound **7a** is an inhibitor, while compounds **8a**, **8b**, and Mtz are not inhibitors. This effect is related to the bile salt export pump (BSEP), expressed almost exclusively in the liver, whose inhibition is associated with hepatotoxicity. BSEP inhibition can result in the accumulation of bile salts in the liver, leading to the induction of liver injury. In our case, the most active compounds do not exhibit possibilities to inhibit BSEP and thus induce potential hepatotoxicity, except for compound **7a**.

Regarding the influence of the studied compounds on the inhibition of CYP450 enzymes, there is a prediction of interference in the metabolism of xenobiotics processed by the isoforms CYP1A2, CYP2C19, CYP2C9, CYP3A4, and CYP2D6. With the exception of compounds **4**, **6**, **7b**, **7c**, **10b**, and Mtz, the others could act as inhibitors of at least one of these enzymatic isoforms, thus reducing the metabolism of their substrates (Table 3, Supplementary information). The inhibition of the CYPs isoforms may lead to inefficient or toxic effects of drugs. The metabolism

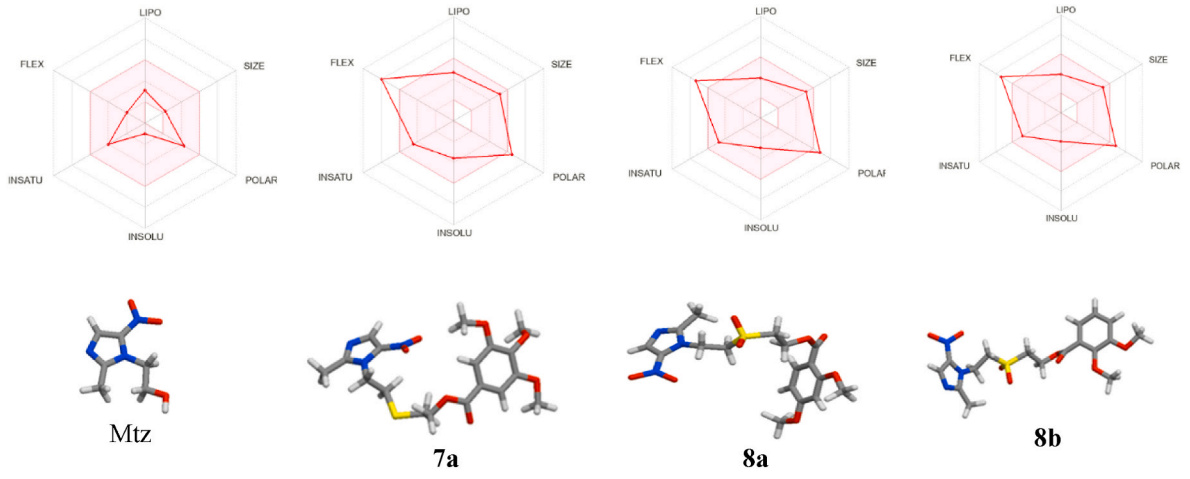

Fig. 5. Bioavailability radar of the compounds Mtz, **7a**, **8a**, and **8b**. In bioavailability radar, the pink area represents the optimal range for each property for oral bioavailability. Lipophilicity (LIPO): XLOGP3 between +1.38 and + 2.62, Mtz −0.02, molecular weight (SIZE): MW between 425 and 427, Mtz 171 g/mol, polarity (POLAR) TPSA between 142 and 150, Mtz 83 $Å^2$, solubility (INSOLU): log S not higher than 1, saturation (INSATU): fraction of carbons in the sp3 hybridization not less than 0.40, Mtz 0.50, and flexibility (FLEX): no more than twelve rotatable bonds.

Table 2
Water solubility of compounds **7a**, **8a**, and **8b**.

Solubility Predictor	7a	8a	8b
Log S (ESOL)	−3.62	−2.91	−2.91
Solubility	2.41 x 10^{-4} M	1.22 x 10^{-3} M	1.22 x 10^{-3} M
Class	Soluble	Soluble	Soluble
Log S (Ali)	−5.27	−4.15	−4.15
Solubility	5.35 x 10^{-6} M	7.04 x 10^{-5} M	7.04 x 10^{-5} M
Class	Moderately Soluble	Moderately soluble	Moderately soluble
Log S (SILICOS-IT)	−4.88	−4.56	−4.56
Solubility	1. x 10^{-5} M	2.75 x 10^{-5} M	2.75 x 10^{-5} M
Class	Moderately soluble	Moderately soluble	Moderately soluble

Log S (ESOL): Estimated SOLubility; Log S (Ali): Topological method; Log S. (SILICOS-IT): Fragmental method calculated FILTER-IT program.

Table 3
Antiproliferative activity (%) of compounds **7a–d**, **8a–c**, **10a–h**, Mtz, Bnz, Nfx, and Aph-B (50 μM) after 72 h of incubation with *T. cruzi* epimastigotes and *L. donovani* promastigotes, IC_{50} μM, and toxicity CC_{50} μM Vero cells for compounds more actives.

No	T. cruzi	L. donovani	IC50 μM T. cruzi	IC50 μM L. donovani	CC50 (μM) Vero cells	SI*
	% Inhibition ±SD					
7a	78.42 ± 2.31	48.54 ± 10.67	7.63 ± 2.32	nd	>300	>39.31
7b	28,60 ± 2.42	25.69 ± 11.55	nd	nd	nd	
7c	40,50 ± 2.02	67,87 ± 6,77	nd	50.37 ± 6.77	nd	
7d	58,57 ± 11.72	35.59 ± 9.75	nd	nd	nd	
8a	93,43 ± 1.62	40.86 ± 5.97	33.86 ± 8.35	nd	nd	
8b	100.0 ± 0.00	71.54 ± 5,15	10.88 ± 1.71	26.31 ± 5.15	>300	>27.57
8c	34.28 ± 3.44	40.29 ± 9.39	nd	nd	nd	
10a	7.57 ± 1.01	26.1 ± 16.63	nd	nd	nd	
10b	47.52 ± 2.73	57.41 ± 5.99	nd	21.9 ± 5.99	>200	
10c	42.71 ± 11.52	34.25 ± 14.0	nd	nd	nd	
10d	47.29 ± 5.45	23.98 ± 4.93	nd	nd	nd	
10e	36.57 ± 3.23	20.16 ± 4.13	nd	nd	nd	
10f	23.71 ± 10.90	16.88 ± 6.02	nd	nd	nd	
10g	10.29 ± 2.02	24.61 ± 5.03	nd	nd	nd	
10h	1.39 ± 0.61	6.70 ± 4.79	nd	nd	nd	
Mtz	12,18 ± 5,30	–	nd	nd	nd	
Bnz	45,39 ± 6,21	–	35,72 ± 1.91	–	>200	
Nfx	83,00 ± 1,60	–	1,81 ± 0.45	–	8.07	
Aph	–	62,44 ± 6,6	–	0,33 ± 0.02	>250	

IC_{50}: Half maximal inhibitory concentration (n = 3); CC_{50}: Half maximal cytotoxicity concentration; SD: Standard deviation; nd: Not determined. SI*: Selectivity index epimastigote forms of *T. cruzi*.

was estimated using the web tool *pkCSM-pharmacokinetics* [34,38,39]. It should be noted that some of the properties calculated by these programs do not always match real experiment values and are only used as indicators in early development work.

2.3. Biology

The biological activity of compounds **7a-d**, **8a-c**, and **10a-h** was determined by measuring their inhibitory capacity on the proliferation of *T. cruzi* epimastigotes, amastigotes and *L. donovani* promastigotes *in vitro* using the MTT technique, the results are reported in Table 3. It is evident that the sulfanyl and sulfonyl benzoate 5-nitroimidazole adducts **7a**, **8a**, and **8b** are more potent trypanocidals against epimastigotes of *T. cruzi* than the parent drugs Mtz, Bnz, and Nfx. The most active adducts, with the best selectivity, were found to be **7a** (IC_{50} 7.63 μM, SI > 39) and **8b** (IC_{50} 10.88 μM, SI > 26) compared to Bnz (IC_{50} 1.81 ± 0.45 μM, SI 8.07). The spacer between the phenyl ring and 5-nitroimidazole core, as well as the presence of methoxy groups appears to have a significant impact on activity. Additionally, the position of the electron-donor substituent on the aromatic ring influences activity, with ortho and meta positions being more favored. The incorporation of an amide functional group as a binding group between 5-nitroimidazol and the phenyl group decreases potency in the evaluated pathologies. However, the presence of two methyl groups in the phenyl ring favors a moderate leishmanicidal effect, as exemplified by compound **10b** (IC_{50} 21.9 μM, SI > 200) compared to Aph (IC_{50} 0,33 ± 0.02 μM, SI > 250). The presence of an oxidized sulfur atom together with the incorporation of two methoxy groups in the orto-meta positions of the phenyl ring produces a moderate leishmanicidal effect as observed for compound **8b** (26.31 μM, SI > 11.4).

Considering the effective inhibition of compound **7a** and **8b** on the

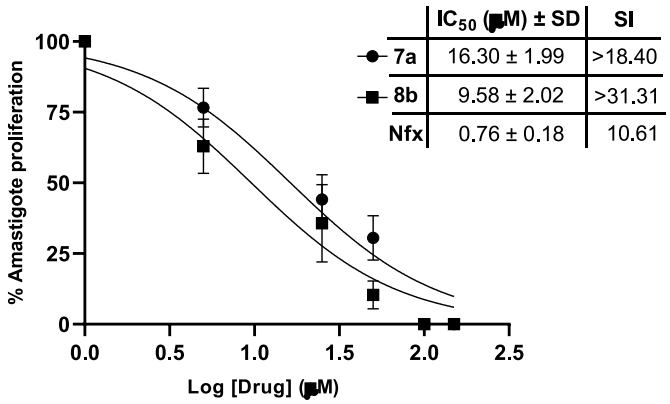

Fig. 6. Effect of **7a** and **8b** on *T. cruzi* amastigotes proliferation.
IC_{50}: Half maximal inhibitory concentration; SD: Standard deviation.
SI: CC_{50} Vero cells/IC_{50} amastigote forms of *T. cruzi*.

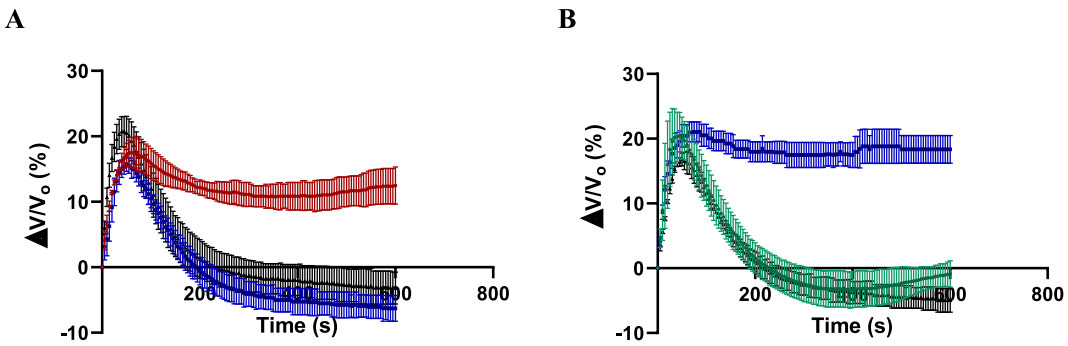

Fig. 7. A. Effects of **7a** (red curve) and **8b** (blue curve) on regulatory volume decrease in *T. cruzi* epimastigotes. **B**. Effects of **10b** (green curve) and **8b** (blue curve) on regulatory volume decrease in *L. donovani* promastigotes.

extracellular stage of *T. cruzi*, their antiparasitic activity was assessed using infected Vero cells. Following a 96-h incubation with these compounds, the percentage of infected cells significantly decreased compared to the non-infected control. Compound **8b** was more active against intracellular amastigotes, had the highest SI (31.31) and lower IC_{50} value (9.58 ± 2.02 μM) and **7a** exhibit an IC_{50}:16.30 ± 1.99 μM with a selectivity index (SI) greater than 18.40 (Fig. 6). A critical requirement in chemotherapeutic research is the absence of host cell toxicity. The most promising derivatives, **7a**, **8b**, and **10b**, exhibited no cytotoxic effects on Vero cells at concentrations that effectively eliminated 50 % of the parasites.

According to the established criteria of the GHIT Fund [40], which requires a half-maximal inhibitory concentration (IC_{50}) <10 μM against intracellular *Trypanosoma cruzi* and an SI > 10, compound **8b** would be considered a *hit* compound and a potential lead compound candidate.

2.4. Osmoregulation assay

T. cruzi responds to hypoosmotic stress by regulating its cell volume through the contractile vacuole complex (CVC). This process involves the efflux of various ions and osmolytes, followed by water release through the contractile vacuole complex [41].

After treating *T. cruzi* epimastigotes and *L. donovani* promastigotes with the most bioactive compounds at IC_{50} concentrations, we evaluated their effect on cellular volume regulation. The parasites were subjected to osmotic changes, and absorbance variations were measured over time as an indicator of cellular volume fluctuations. The results demonstrate an increase in cellular volume when these parasites are exposed to hypoosmotic stress (150 mOsm/L), as evidenced in Fig. 7. Analysis of the recovery rate between 100 and 400 s revealed significant differences: epimastigotes treated with **7a** failed to recover their normal volume even after 600 s, maintaining a residual volume change of approximately 16 %. Parasites treated with **8b** recovered their cellular volume within 200 s, similar to the control group (Fig. 7A). In contrast, promastigotes treated with this compound did not recover their cellular volume, showing a maximum change of approximately 23 % compared to the control group's 17 % change. Those treated with **10b** successfully recovered their initial volume, matching the hypoosmotic control (Fig. 7B). From a morphological perspective, it should be noted that an oncotic cell is undergoing necrotic cell death, though additional markers are necessary for confirmation.

3. Conclusions

Among the fifteen new 5-nitroimidazole hybrids being reported, two compounds **7a** and **8b** were active against the epimastigote form of *T. cruzi*. Compound **10b** showed marginal activity against the promastigote form of *L. donovani*. Considering the effective inhibition of compound **7a** and **8b** on the extracellular stage of *T. cruzi*, their antiparasitic activity was assessed using infected Vero cells. Of the two most active compounds, sulfonyl derivative **8b** was the most promising compound, with good potency (IC_{50}: 9.58 ± 2.02 μM) and with a selectivity index (SI) greater than 31.31, that justifies the description as a promising hit for further study as a possible antichagasic agent. Initial observations on SARs suggested that, among the compounds prepared, the one containing an ethyl sulfonyl benzoate, with positions 2,3 occupied with methoxy groups, is the most active, while its analogous amides exhibit marginal activity as trypanocides and leishmanicides. The hypothesis could be related to the ability of the amide and hydroxyl groups to favor a strong binding to proteins that may be reducing the ability of these molecules to cross the membranes of the parasites efficiently, a deduction that is made from the theoretical values obtained for the descriptor of total clearance (CLtot) of the synthesized compounds ranged from 0.344 to 0.819 ml/min/kg, being the one presented for compound **8b** of 0.373 ml/min/kg. Value achieved of log S (ESOL) of −2.91 by compound **8b** help us predict that the intraperitoneal route should be the best way to achieve a positive antiparasitic effect. ADME/Tox analysis predicted for more active compound **8b**, indicate that it is not hepatotoxic and with respect to LD_{50}, it is less lethal than Mtz. From the morphological point of view, it must be taken into account that an oncotic cell is suffering a necrotic death, in the case of the treatment of *L. donovani* promastigotes with compound **8b**, however in the case of *T. cruzi* treatments with **8b** the same behavior was not observed. Additional markers will be needed for confirmation. Compounds 5-nitroimidazole hybrids were obtained, each from a five-steps synthetic pathway, from commercially available precursors with overall yields of up to 60 % in most cases. All compounds were characterized by IR, ^{1}HNMR, ^{13}CNMR, Mass spectrometric analysis, and by elemental analysis.

4. Experimental

4.1. Chemicals and instrumentation

FTIR spectroscopy was determined on a PerkinElmer™ Spectrum two using a Diamon/ZnSe attenuated total reflectance (ATR) sampling accessory. Readings were taken at rt, 64 scans/min per analysis, resolution of 0.5 cm^{-1}, range from 4000 to 450 cm^{-1}. The ^{1}H and ^{13}C NMR spectra were performed using a spectrometer Nanalysis™ 100 MHz PRO Benchtop and a JEOL™ Eclipse 270 spectrometer (at 100 and 270 MHz for ^{1}H and 25.8 and 67.9 MHz for ^{13}C) using $CDCl_3$ as the solvent, and are reported in ppm downfield from the residual $CHCl_3$ δ 7.25 for ^{1}H NMR and 77.0 for ^{13}C NMR, respectively. Mass spectra were recorded with an Agilent™ GCMS model 5977C spectrometer in EI (70 eV) coupled directly to na Angilet™ model 8860 gas chromatograph. Elemental analyses were achieved using a Perkin Elmer™ 2400 CHN elemental analyzer, and the results were within ±0.4 % of the predicted values. Melting points were determined on a Fisher-Johns™ fusiometer and are not corrected. Thin-layer chromatography (TLC) was carried out

on Merck™ silica F254 0.255-mm plates, and spots were visualized by UV fluorescence at 254 nm. Chemical reagents were obtained from Aldrich Chemical Co™, USA. All solvents were distilled and dried in the usual manner. Compounds **3**, **4**, **6**, **7a-d**, and **8a-c** were reported previously [19,25,28].

*4.1.1. General procedure for synthesis of final compounds 2-{[2-(2-methyl-5-nitro-1H-imidazole-1-yl)ethyl]thio}-N-phenylacetamide derivatives **10a-h***

A mixture of 0.03 mmol of **6** in 5 mL of dry dimethylformamide (DMF) was stirred to rt for 10 min, then 1-Ethyl-3-(3-dimethylaminopropyl)carbodiimide hydrochloride (EDCI) 0.03 mmol was added, the resulting mixture was stirred at 0 °C for 30 min, then 4-dimethylamine pyridine (DMAP) 5 % and corresponding aniline **9a-h** 0.03 mmol dissolved in 2 mL of dry DMF were added. The reaction mixture was left under an inert atmosphere at rt and constant agitation for 12 h. After this time, a portion of 10 mL of distilled water and 10 mL of saturated $NaHCO_3$ solution were added, extracted with two portions of 50 mL of AcOEt. The organic layers were joined and washed with two 50 mL portions of distilled water, one 50 mL portion of saturated NaCl solution, and dried with anhydrous Na_2SO_4, filtered and removed solvent at reduced pressure. The resulting solid was washed with 10 mL of ethyl ether and dried in a vacuum oven at 40 °C for 24 h. The compounds of interest were obtained by purifying them by column chromatography (Cyclohexane:EtOAc 1:1).

*4.1.1.1. N-(3-methoxyphenyl)-2-{[2-(2-methyl-5-nitro-1H-imidazole-1-yl)ethyl]thio}acetamide **10a**.* Yellow solid; yield 76 %; mp. 128–130 °C; IR cm^{-1}: 3206, 3153, 3064, 2923, 1673, 1613, 1595, 1563, 1532, 1466, 1422, 1370; ^{1}H RMN ($CDCl_3$, 270 MHz) δ: 2.50 (s, 3H, CH_3), 2.98 (t, 2H, H_7, $J = 7$ Hz), 3.34 (s, 2H, H_9), 3.78 (s, 3H, OCH_3), 4.51 (t, 2H, H_6, $J = 7$ Hz), 6.66 (d, 1H, $H_{4'}$, $J = 8$ Hz), 6.99 (d, 1H, $H_{6'}$, $J = 8$ Hz), 7.19 (d, 1H, $H_{5'}$, $J = 8$ Hz), 7.25 (s, 1H, $H_{2'}$), 7.99 (brs, 1H, NH), 8.20 (s, 1H, H_4). ^{13}C NMR ($CDCl_3$, 67.9 MHz) δ 14.2 ($2CH_3$), 32.2 (C_7), 36.9 (C_9), 45.5 (C_6), 55.4 (OCH_3), 105.7 ($C_{2'}$), 110.7 ($C_{4'}$), 111.9 ($C_{6'}$), 129.9 ($C_{5'}$), 138.3 (C_5), 166.5 (C=O); (EI) *m/z* (%): 350.10 [M^+] (3.3), 195.03 [$M^+ - C_9H_{10}NO_2S$] (4.9), 165.08 [$M^+ - C_9H_{11}NO_2$] (53), 123.06 [$M^+ - C_7H_9NO$] (100). Anal. Calcd for $C_{15}H_{18}N_4O_4S$: C, 51.42; H, 5.18; N, 15.99. Found: C, 51.40; H, 5.23; O, 16.27.

*4.1.1.2. N-(4-methoxyphenyl)-2-{[2-(2-methyl-5-nitro-1H-imidazole-1-yl)ethyl]thio}acetamide **10b**.* Yellow solid; yield 65 %; mp. 124–126 °C; IR cm^{-1}: 3239, 3187, 3036, 1667, 1608, 1550, 1535, 1511, 1469, 1389, 1362; ^{1}H NMR ($CDCl_3$, 270 MHz) δ: 2.51 (s, 3H, CH_3), 2.98 (t, 2H, H_7, $J = 7$ Hz), 3.34 (s, 2H, H_9), 3.77 (s, 3H, OCH_3), 4.52 (t, 2H, H_6, $J = 7$ Hz), 6.85 (d, 2H, $H_{3',5'}$, $J = 9$ Hz), 7.40 (d, 2H, $H_{2',6'}$, $J = 9$ Hz), 7.92 (s, 1H, H_4), 8.11 (brs, 1H, NH). ^{13}C NMR ($CDCl_3$, 67.9 MHz) δ: 14.4 (CH_3), 32.2 (C_7), 36.8 (C_9), 45.5 (C_6), 55.6 (OCH_3), 114.4 ($C_{3',5'}$), 121.8 ($C_{2',6'}$), 130.4 ($C_{1'}$), 133.3 (C_4), 138.5 (C_5), 150.5(C_2), 157.0 ($C_{4'}$), 166.3 (C=O). (EI) *m/z* (%): 350.10 [M^+] (8.2), 195.04 [$M^+ - C_9H_{10}NO_2S$] (15), 165.07 [$M^+ - C_9H_{11}NO_2$] (40), 123.06 [$M^+ - C_7H_9NO$] (61), 108.04 [$M^+ - C_7H_8O$] (100). Anal. Calcd for $C_{15}H_{18}N_4O_4S$: C, 51.42; H, 5.18; N, 15.99. Found: C, 51.47; H, 5.31; O, 16.18.

*4.1.1.3. N-(benzo[d] [1,3]dioxol-5-yl)-2-{[2-(2-methyl-5-nitro-1H-imidazole-1-yl)ethyl]thio}- acetamide **10c**.* Brown solid; yield 82 %; mp. 132–134 °C; IR cm^{-1}: 3263, 3222, 3075, 1671, 1641, 1569, 1535, 1488, 1379, 1368; ^{1}H NMR ($CDCl_3$, 270 MHz) δ: 2.51 (s, 3H, CH_3), 2.98 (t, 2H, H_7, $J = 7$ Hz), 3.32 (s, 2H, H_9), 4.51 (t, 2H, H_6, $J = 7.2$ Hz), 5.93 (s, 2H, OCH_2O), 6.72 (d, 1H, $H_{5'}$, J = 8 Hz), 6.79 (dd, 1H, $H_{6'}$, $J = 8$, 2 Hz), 7.20 (d, 1H, $H_{2'}$, $J = 2$ Hz), 7.92 (s, 1H, H_4), 8.16 (brs, 1H, NH). ^{13}C NMR ($CDCl_3$, 67.9 MHz) δ: 14.4 (CH_3), 32.2 (C_7), 36.8 (C_9), 45.5 (C_6), 101.4 (O-CH_2-O), 102.7 ($C_{2'}$), 108.1 ($C_{6'}$), 113.2 ($C_{5'}$), 131.5 ($C_{1'}$), 133.3 (C_4), 138.5 (C_5), 144.8 ($C_{4'}$), 148.0 ($C_{3'}$), 150.5(C_2), 166.3 (C=O). (EI) *m/z* (%): 364.07 [M^+] (8.4), 209.03 [$M^+ - C_9H_8NO_3S$] (18.3), 179.05 [$M^+ - C_9H_9NO_3$] (44.7), 137.05 [$M^+ - C_7H_7NO_2$] (100 %). Anal. Calcd for $C_{15}H_{16}N_4O_5S$: C, 49.44; H, 4.43; N, 15.38. Found: C, 49.63; H, 4.41; N, 15.27.

*4.1.1.4. N-(3,5-dimethylphenyl)-2-{[2-(2-methyl-5-nitro-1H-imidazole-1-yl)ethyl]thio}acetamide **10d**.* White solid; yield 93 %; mp. 133–135 °C; IR cm^{-1}: 3305, 3211, 3153, 3064, 3022, 1673, 1613, 1563, 1532, 1466, 1422, 1381, 1370. ^{1}H NMR ($CDCl_3$, 270 MHz) δ: 2.28 (s, 6H, 2 x CH_3), 2.51 (s, 3H, CH_3), 2.98 (t, 2H, H_7, $J = 7$ Hz), 3.34 (s, 2H, H_9), 4.52 (t, 2H, H_6, $J = 7$ Hz), 6.77 (s, 1H, $H_{4'}$), 7.13 (s, 2H, $H_{2',6'}$), 7.92 (s, 1H, H_4), 8.06 (brs, 1H, NH). ^{13}C NMR ($CDCl_3$, 67.9 MHz) δ: 14.4 (CH_3), 21.4 (2 x CH_3), 32.2 (C_7), 37.0 (C_9), 45.5 (C_6), 117.6 ($C_{2',6'}$), 126.7 ($C_{4'}$), 133.2 (C_4), 137.1 ($C_{1'}$), 139.0 ($C_{3',5'}$), 150.5 (C_2), 166.3 (C=O). (EI) *m/z* (%): M^+ 348.10 [M^+] (1.9), 193.04 [$M^+ - C_{10}H_{12}NOS$] (4), 163.09 [$M^+ - C_{10}H_{12}NO$] (37), 121.09 [$M^+ - C_8H_{10}N$] (100). Anal. Calcd for $C_{16}H_{20}N_4O_3S$: C, 55.16; H, 5.79; N, 16.08. Found: C, 55.08; H, 5.83; N, 15.97.

*4.1.1.5. N-(3,5-dichlorophenyl)-2-{[2-(2-methyl-5-nitro-1H-imidazole-1-yl)ethyl]thio}acetamide **10e**.* Yellow solid; yield 74 %; mp. 187–189 °C; IR cm^{-1}: 3242, 3217, 3022, 2992, 1683, 1608, 1587, 1535, 1459, 1435, 1368. ^{1}H NMR ($CDCl_3$, 270 MHz) δ: 2.53 (s, 3H, CH_3), 2.98 (t, 2H, H_7, $J = 7$ Hz), 3.35 (s, 2H, H_9), 4.52 (t, 2H, H_6, $J = 7$ Hz), 7.12 (s, 1H, $H_{4'}$), 7.49 (s, 2H, $H_{2',6'}$), 7.95 (s, 1H, H_4), 8.19 (s, 1H, NH). ^{13}C NMR ($CDCl_3$, 67.9 MHz) δ: 14.4 (CH_3), 32.3 (C_7), 36.8 (C_9), 45.4 (C_6), 118.0 ($C_{2',6'}$), 124.9 ($C_{4'}$), 133.2 (C_4), 135.5 ($C_{3',5'}$), 139.0 (C_5), 167.2 (C=O). (EI) *m/z* (%): 227.02 [$M^+ - C_8H_{10}N_3O_3S$] (5), 199.03 [$M^+ - C_7H_{10}N_3O_2S$] (5), 186.04 [$M^+ - C_6H_8N_3O_2S$] (6), 155.04 [$M^+ - C_6H_8N_3O_2$] (100), 140.05 [$M^+ - C_5H_6N_3O_2$] (30.1). Anal. Calcd for $C_{14}H_{14}Cl_2N_4O_3S$: C, 43.20; H, 3.63; N, 14.39. Found: C, 43.29; H, 3.61; N, 14.22.

*4.1.1.6. N-(4-chloro-2,6-dimethylphenyl)-2-{[2-(2-methyl-5-nitro-1H-imidazole-1-yl)ethyl]thio}-acetamide **10f**.* Yellow solid; yield 63 %; mp. 139–141 °C; IR cm^{-1}: 3218, 3172, 3123, 1625, 1587, 1528, 1487, 1425, 1383, 1361. ^{1}H NMR ($CDCl_3$, 270 MHz) δ: 2.16 (s, 6H, 2 x CH_3), 2.53 (s, 3H, CH_3), 3.05 (t, 2H, H_7, $J = 7$ Hz), 3.37 (s, 2H, H_9), 4.55 (t, 2H, H_6, $J = 7$ Hz), 7.04 (s, 2H, $H_{3',5'}$), 7.63 (brs, 1H, NH), 7.94 (s, 1H, H_4). ^{13}C NMR ($CDCl_3$, 67.9 MHz) δ: 14.4 (CH_3), 18.3 (2 x CH_3), 32.4 (C_7), 35.8 (C_9), 45.4 (C_6), 128.3 ($C_{3',5'}$), 131.9 ($C_{4'}$), 133.0 ($C_{2',6'}$), 133.2 (C_4), 137.1 ($C_{1'}$), 150.5 (C_2), 166.9 (C=O). (EI) *m/z* (%): 382.08 [M^+] (1.9), 228.02 [M + − $C_{10}H_{11}ClNOS$] (5), 197.05 [M + − $C_{10}H_{11}ClNOS$] (26), 155.04 [M + − C_8H_9ClN] (100). Anal. Calcd for $C_{16}H_{19}ClN_4O_3S$: C, 50.19; H, 5.00; N, 14.63. Found: C, 50.32; H, 4.98; N, 14.85.

*4.1.1.7. N-(4-bromo-2,6-dimethylphenyl)-2-{[2-(2-methyl-5-nitro-1H-imidazole-1-yl)ethyl]thio}-acetamide **10g**.* Brown solid; yield 60 %; mp. 128–130 °C; IR cm^{-1}: 3218, 3120, 3019, 1625, 1587, 1528, 1469, 1426, 1361, 1305. ^{1}H NMR ($CDCl_3$, 270 MHz) δ: 2.15 (s, 6H, 2 x CH_3), 2.53 (s, 3H, CH_3), 3.04 (t, 2H, H_7, $J = 7$ Hz), 3.36 (s, 2H, H_9), 4.55 (t, 2H, H_6, $J = 7$ Hz), 7.20 (s, 2H, $H_{3',5'}$), 7.65 (s, 1H, NH), 7.94 (s, 1H, H_4). ^{13}C NMR ($CDCl_3$, 67.9 MHz) δ: 14.4 (CH_3), 18.2 (2 x CH_3), 32.4 (C_7), 35.8 (C_9), 45.4 (C_6), 121.2 ($C_{4'}$), 131.2 ($C_{3',5'}$), 132.4 ($C_{1'}$), 133.3 (C_4), 137.1 ($C_{2',6'}$), 166.9 (C=O). (EI) *m/z* (%): 427.90 [M^+] (2), 272.94 [M + − $C_{10}H_{11}BrNOS$] (10), 241.00 [M + − $C_{10}H_{11}BrNO$] (20), 224.99 [M + − C_9H_9BrNO] (24), 224.99 [M + − C_9H_9BrNO] (24), 198.99 [M + − C_8H_9BrN] (90), 120.07 [M + − C_8H_9N] (100). Anal. Calcd for $C_{16}H_{19}BrN_4O_3S$: C, 44.97; H, 4.48; N, 13.11. Found: C, 45.09; H, 4.47; N, 12.91.

*4.1.1.8. 2-{[2-(2-methyl-5-nitro-1H-imidazole-1-yl)ethyl]thio}-N-(3,4,5-trimethoxyphenyl)-acetamide **10h**.* Brown solid; yield 68 %; mp. 152–154 °C; IR cm^{-1}: 3244, 3203, 3118, 3049, 1678, 1606, 1541, 1506, 1447, 1365, 1309. ^{1}H NMR ($CDCl_3$, 270 MHz) δ: 2.52 (s, 3H, CH_3), 2.99 (brs, 2H, H_7), 3.35 (s, 2H, H_9), 3.80 (s, 3H, 4′OCH_3), 3.84 (s, 6H, 2 x OCH_3), 4.53 (t, 2H, H_6, $J = 7$ Hz), 6.84 (s, 2H, $H_{2',6'}$), 8.02 (brs, 1H, NH),

8.10 (s, 1H, H_4). ^{13}C NMR ($CDCl_3$, 67.9 MHz) δ: 14.4 (CH_3), 32.1 (C_7), 36.9 (C_9), 45.4 (C_6), 56.3 (2 x OCH_3), 61.0 (4′OCH_3), 97.8 ($C_{2',6'}$), 133.4 (C_4), 135.4 ($C_{4'}$), 153.6 ($C_{3',5'}$), 166.3 (C=O). (EI) *m/z* (%): 410.14 [M^+] (22.4), 255.06 [M + − $C_{10}H_{14}NO_4S$], (10), 225.11 [M + − $C_{10}H_{14}NO_4$] (37), 210.07 [M + − $C_{10}H_{12}NO_4$] (18), 183.08 [M + − $C_9H_{12}NO_3$] (14), 168.07 [M + − $C_9H_{11}NO_3$] (100). Anal. Calcd for $C_{17}H_{22}N_4O_6S$: C, 49.75; H, 5.40; N, 13.65. Found: C, 49.75; H, 5.43; N, 13.78.

4.1.2. ADME/Tox profile prediction

To predict the pharmacokinetic and physicochemical properties, toxicity, and drug-likeness of the synthesized molecules were used the *SwissADME* program and *pkCSM-pharmacokinetics,* free online programs available at http://www.swissadme.ch/and http://structure. bioc.cam.ac.uk/pkcsm (accessed on August 17, 2024) [30,34].

4.1.3. In vitro anti-parasitic assay

Trypanosoma cruzi epimastigotes (Y strain (TCII)) were used [42], culture in axenic conditions in liver infusion tryptose (LIT) medium supplemented with 10 % inactivated fetal bovine serum. Cultures were maintained at 28 °C with subcultures performed every week into 25 cm^2 flask. Parasites were harvested in the logarithmic growth phase prior to experiments.

Leishmania donovani promastigotes (LD51 strain) were grown in liver infusion tryptose medium (LIT), with 100 % inactive fetal bovine serum. Parasites were collected in the logarithmic phase of growth before to the experiments.

4.1.4. In vitro evaluation of the effect of derivatives **7a-d, 8a-c,** and **10a-h** on the proliferation of T.cruzi epimastigotes byMTT assay

Epimastigotes (2 x 10^5 per well) were seeded in 96-well plates and incubated at 28 °C for 24 h, the compounds to be evaluated, dissolved in DMSO (0.1 % final concentration), were then added at a single concentration of 50 μM. A drug-free control (negative control) was included, and benznidazole and nifurtimox were used as positive controls. After 72 h of incubation with the test compounds, MTT (5 mg/mL in PBS) was added and incubated for 4 h in the dark. Finally, cells were lysed with DMSO, and the absorbance was measured at 570 nm using a spectrophotometer [43,44].

4.1.5. In vitro evaluation of the effect of derivatives **7a-d, 8a-c,** and **10a-h** on the proliferation of L. donovani promastigotes by MTT assay

Promastigotes (4 x 10^5 per well) were seeded in 96-well plates and incubated at room temperature for 24 h. The compounds to be evaluated, dissolved in DMSO (0.1 % final concentration), were then added at a single concentration of 50 μM, a drug-free control (negative control) was included, and amphotericin B was used as leishmanicidal control. After 72 h of incubation with the test compounds, MTT (5 mg/mL in PBS) was added and incubated for 4 h in the dark. Finally, the cells were lysed with DMSO, and the absorbance was measured at 570 nm using a spectrophotometer [44].

4.1.6. Estimation of half maximal inhibitory concentration (IC_{50}) of derivatives **7a, 8a-b** againts T. cruzi epimastigotes and L. donovani promastigotes

T. cruzi epimastigotes (2x10^5 parasites per well) or *L. donovani* promastigotes (4x10^5 per well) were seeded in 96-well plates and incubated at 28 °C for 24 h. Compounds 7a, 8a and 8b as well as the reference drugs, benznidazole, nifurtimox and amphotericin B, dissolved in DMSO (0.1 % final concentration were tested in triplicate at concentrations ranging from 10 to 100 μM. Growth inhibition was assessed after 72 h of incubation in the presence of the compounds using MTT (5 mg/mL in PBS), incubated for 4 h in the dark. Finally, parasites were lysed with DMSO, and the absorbance was measured at 570 nm using a spectrophotometer.

4.1.7. In vitro evaluation of derivatives **7a** and **8b** effects on T. cruzi intracelular amastigotes proliferation

For the intracellular amastigote experiment, Vero E6 cells (ATCC No. CRL-1586) were cultured in 12-well plates (4x10^5 cells/mL) containing coverslips in DMEM supplemented with 10 % fetal bovine serum, and incubated at 37 °C in a humidified 5 % CO_2 atmosphere. Subsequently, the cells were infected with *T. cruzi* trypomastigotes (10:1 ratio, parasite/cell). After 12 h of infection, cells were washed with PBS to remove non-internalized parasites. Compounds **7a** and **8b**, dissolved in DMSO (0.1 % final concentration), were tested in triplicate at concentrations ranging from 5 to 150 μM. Nifurtimox was used as reference drugs at concentration range from 0.5 to 8 μM. Plates were incubated for 96 h at 37 °C in in a humidified 5 % CO_2 atmosphere. Coverslips were analyzed under light microscopy, and the number of infected cells were determinate. The results were expressed as the percentage of amastigotes proliferation compared to that of untreated control wells, the 50 % inhibitory concentration (IC_{50}) was calculated using non-linear regression in Prism (GraphPad).

4.1.8. Host cell totoxicity assay

To determine the potential toxic effects of the compounds on the host cells, uninfected Vero cells were used. Cells were maintained in DMEM supplemented with 10 % fetal bovine serum, and incubated at 37 °C in a humidified 5%CO_2 atmosphere. Cells were counted in suspension using a Neubauer chamber and seeded at 2 x 10^4 cells/well in 96-well plate. After 24 h, compounds were added. Cells viability was measured after 48 h using the MTT [3-(4,5-Dimethyl-2-thiazolyl)-2,5-Diphenyl-2H-tetrazolium bromide] colorimetric assay. MTT (5 mg/mL) was added and incubated in darkness for 4 h. After this time, DMSO was added, and the absorbance was measured at 540 nm using a Synergy HT spectrophotometer (Biotek). The assay was performed in triplicate at different concentrations: 5, 15, 25, 50, 100, 200 and 300 μM, including untreated cells and reference drug controls [44].

4.1.9. Cell volume regulation assay

The assays were performed according to the method reported by Schoijet et al. [45], with minor modifications. Epimastigote cultures were centrifuged at 5000 g and washed twice with isotonic chloride buffer (ISO-Cl buffer: 137 mM NaCl, 4 mM KCl, 1.5 mM KH_2PO_4, 8.5 mM Na_2HPO_4, 20 mM HEPES, 11 mM glucose, 1 mM $CaCl_2$, 0.8 mM $MgSO_4$, pH 7.4). The buffer osmolarity was adjusted to 300 ± 5 mOsm. Subsequently, parasites were resuspended in ISO-Cl buffer at a density of 1 x 10^8 parasites/mL. The parasites were then dispensed into 96-well plates at a concentration of 1 x 10^8 parasites/mL/well in a total volume of 100 μL/well, in triplicate. To evaluate the effect of the compounds on cell volume regulation capacity, hypoosmotic stress was induced by adding 100 μL of sterile deionized water to each well. Changes in absorbance, proportional to cell swelling, were measured every 5 s for 10 min at 550 nm using an ELISA plate reader.

CRediT authorship contribution statement

Miguel A. Rodríguez: Methodology, Investigation. **Ali Mijoba:** Methodology, Investigation. **Nereida J. Parra-Giménez:** Validation, Supervision, Project administration, Conceptualization. **Zuleyma Blanco:** Methodology, Investigation. **Katiuska Chávez:** Investigation, Formal analysis. **Alirica I. Suárez:** Supervision, Formal analysis. **Esteban Fernandez-Moreira:** Writing – original draft, Supervision, Formal analysis, Conceptualization. **Hegira Ramírez:** Writing – original draft, Visualization, Supervision, Investigation, Formal analysis. **Jaime E. Charris:** Writing – review & editing, Writing – original draft, Supervision, Resources, Formal analysis, Conceptualization.

Data availability

The supporting data for the conclusions of this study can be found in

the supplementary material provided with this article.

Funding

The authors acknowledge the financial support from the Ministerio de Ciencia, Tecnología e Innovación de Venezuela (grant numbers 20240PGP82 and 20220PGP65).

Declaration of competing interest

The authors declare the following financial interests/personal relationships which may be considered as potential competing interests: JAIME ENRIQUE CHARRIS CHARRIS reports financial support, article publishing charges, equipment, drugs, or supplies, and travel were provided by Gobierno de la República Bolivariana de Venezuela Ministerio de Ciencia y Tecnología. JAIME ENRIQUE CHARRIS CHARRIS reports a relationship with No interest to reveal that includes: employment. No patents to disclose has patent No patents to disclose pending to No patents to disclose. Don't exiets anything else that can influence If there are other authors, they declare that they have no known competing financial interests or personal relationships that could have appeared to influence the work reported in this paper.

Acknowledgements

The authors acknowledge the Instituto de Investigaciones Farmacéuticas de la Facultad de Farmacia, Universidad Central de Venezuela.

Appendix A. Supplementary data

Supplementary data to this article can be found online at https://doi.org/10.1016/j.ejmcr.2025.100248.

Data availability

No data was used for the research described in the article.

References

[1] Ending the Neglect to Attain the Sustainable Development Goals: a Road Map for Neglected Tropical Diseases 2021-2030, World Health Organization, Geneva, 2020. License: CC BY-NC-SA 3.0 IGO, https://www.who.int/publications/i/item/9789240010352.
[2] J. Martín-Escolano, C. Marín, M.J. Rosales, A.D. Tsaousis, E. Medina-Carmona, R. Martín-Escolano, An updated view of the *Trypanosoma cruzi* life cycle: intervention points for an effective treatment, ACS Infec. Dis. 8 (2022) 1107–1115, https://doi.org/10.1021/acsinfecdis.2c00123.
[3] W.J.S. Mota, B.N. Guedes, S. Jain, J.C. Cardoso, P. Severino, E.B. Souto, Classical and innovative drugs for the treatment of Leishmania infections, Discov. Public Health 21 (2024) 122, https://doi.org/10.1186/s12982-024-00247-1.
[4] K.C.F. Lidani, F.A. Andrade, L. Bavia, F.S. Damasceno, M.H. Beltrame, I.J. Messias-Reason, T.L. Sandri, Chagas disease: from discovery to a worldwide health problem, Front. Public Health 7 (2019) 166, https://doi.org/10.3389/fpubh.2019.00166.
[5] Symptoms, transmission, and current treatments for Chagas disease DNDi. https://dndi.org/diseases/chagas/facts/, 2020. March 2024.
[6] V. Ribeiro, N. Dias, T. Paiva, L. Hagström-Bex, N. Nitz, R. Pratesi, M. Hecht, Current trends in the pharmacological management of Chagas disease, Int. J. Parasitol. Drugs Drug Resist. 12 (2020) 7–17, https://doi.org/10.1016/j.ijpddr.2019.11.004.
[7] Fexinidazole for Chagas DNDi. https://dndi.org/research-development/portfolio/fexinidazole-chagas/, 2020. March 2024.
[8] F. Torrico, J. Gascón, L. Ortiz, J. Pinto, G. Rojas, A. Palacios, F. Barreira, B. Blum, A.G. Schijman, M. Vaillant, N. Strub-Wourgaft, M.-J. Pinazo, G. Bilbe, I. Ribeiro, A phase 2, randomized, multicenter, placebo-controlled, proof of concept trial of oral fexinidazole in adults with chronic indeterminate Chagas Disease, Clin. Infect. Dis. 76 (2023) e1186–e1194, https://doi.org/10.1093/cid/ciac579.
[9] S. Burza, S.L. Croft, M. Boelaert, Leishmaniasis, Lancet 392 (2018) 951–970, https://doi.org/10.1016/S0140-6736(18)31204-2.
[10] R.C. Zauli-Nascimento, D.C. Miguel, J.K. Yokoyama-Yasunaka, L.I. Pereira, M. A. Pelli de Oliveira, F. Ribeiro-Dias, M.L. Dorta, S.R.B. Uliana, In vitro sensitivity of *Leishmania* (Viannia) braziliensis and Leishmania (Leishmania) amazonensis Brazilian isolates to meglumine antimoniate and amphotericin B, Trop. Med. Int. Health 15 (2010) 68–76, https://doi.org/10.1111/j.1365-3156.2009.02414.x.
[11] S.L. Croft, S. Sundar, A.H. Fairlamb, Drug resistance in leishmaniasis, Clin. Microbiol. Rev. 19 (2006) 111–126, https://doi.org/10.1128/CMR.19.1.111-126.2006.
[12] J. Chakravarty, S. Sundar, Drug resistance in leishmaniasis, J. Glob. Infect. Dis. 2 (2010) 167–176, https://doi.org/10.4103/0974-777X.62887.
[13] A.B. Vermelho, G.C. Rodrigues, C.T. Supuran, Why hasn't there been more progress in new Chagas disease drug discovery? Expert Opin. Drug Discov. 15 (2019) 145–158, https://doi.org/10.1080/17460441.2020.1681394.
[14] K.T. Andrews, G. Fisher, T.S. Skinner-Adams, Drug repurposing and human parasitic protozoan diseases, Int. J. Parasitol. Drugs Drug Resist. 4 (2014) 95–111, https://doi.org/10.1016/j.ijpddr.2014.02.002.
[15] E.O.J. Porta, S.N. Jäger, I. Nocito, G.I. Lepesheva, E.C. Serra, B.L. Tekwani, G. R. Labadie, Antitrypanosomal and antileishmanial activity of prenyl-1,2,3-triazoles, MedChemComm 8 (2017) 1015–1021, https://doi.org/10.1039/C7MD00008A.
[16] A. Bhattacharya, A. Corbeil, R.L. do Monte-Neto, C. Fernandez-Prada, Of Drugs and Trypanosomatids: new tools and knowledge to reduce bottlenecks in drug discovery, Genes 11 (2020) 722, https://doi.org/10.3390/genes-11070722.
[17] P. García-Huertas, N. Cardona-Castro, Advances in the treatment of Chagas disease: promising new drugs, plants and targets, Biomed. Pharmacother. 142 (2021) 112020, https://doi.org/10.1016/j.biopha.2021.112020.
[18] P.M. Wright, I.B. Seiple, G. Myers, The evolving role of chemical synthesis in antibacterial drug discovery, Angew. Chem. Int. Ed. 52 (2014) 8840–8869, https://doi.org/10.1002/anie.201310843.
[19] Z. Blanco, M.R. Mijares, H. Ramírez, E. Fernandez-Moreira, H.J. Oviedo, N. M. Rodríguez, J.E. Charris, *In vitro* evaluation and *in vivo* efficacy of nitroimidazole-sulfanyl ethyl derivatives against *Leishmania* (V.) *braziliensis* and *Leishmania* (L.) *mexicana*, Parasitol. Res. 120 (2021) 3307–3317, https://doi.org/10.1007/s00436-021-07266-w.
[20] C.W. Ang, A.M. Jarrad, M.A. Cooper, M.A.T. Blaskovich Nitroimidazoles, Molecular fireworks that combat a broad spectrum of infectious diseases, J. Med. Chem. 60 (2017) 7635–7657, https://doi.org/10.1021/acs.jmedchem.7b00143.
[21] F.V.C.E. Mello, B.M. Castro Salomão Quaresma, M.C. Resende Pitombeira, M. Araújo de Brito, P.P. Farias, S. Lisboa de Castro, K. Salomão, A. Silva de Carvalho, J.I. Oliveira de Paula, S. de Brito Nascimento, M. Peixoto Cupello, M. C. Paes, N. Boechat, I. Felzenszwalb, Novel nitroimidazole derivatives evaluated for their trypanocidal, cytotoxic, and genotoxic activities, Eur. J. Med. Chem. 185 (2020) 111887, https://doi.org/10.1016/j.ejmech.2019.111887.
[22] A. Upadhyay, P. Chandrakar, S. Gupta, N. Parmar, S. Kumar Singh, M. Rashid, P. Kushwaha, M. Wahajuddin, K.V. Sashidhara, S. Kar, Synthesis, biological evaluation, structure-activity relationship, and mechanism of action studies of quinoline-metronidazole derivatives against experimental visceral leishmaniasis, J. Med. Chem. 62 (2019) 5655–5671, https://doi.org/10.1021/acs.jmedchem.9b00628.
[23] M.F. Pelozo, G.F. Serpa Lima, C.F. Cordeiro, L.S. Silva, I.S. Caldas, D. Teixeira Carvalho, S. Neiva Laborato, J.A. Haekes, L. Lopardi Franco, Synthesis of new hybrid derivatives from metronidazole and eugenol analogues as trypanocidal agents, J. Pharm. Pharm. Sci. 24 (2021) 421–434, https://doi.org/10.18433/jpps31839.
[24] A.C. Manoel Von Trompowsky, T. Ramos Conde, R. Calil Lemos, B.M. Castro Salomão Quaresma, M.C. Sr Pitombeira, A. Silva de Carvalho, N. Boechat, K. Salomão, S. Lisboa de Castro, H. Pereira da Silva Zamith, In vitro genotoxicity of nitroimidazoles as a tool in the search of new trypanocidal agents, Mem. Inst. Oswaldo Cruz 114 (2019) e190017, https://doi.org/10.1590/0074-02760190017.
[25] M. Rodríguez, J. Gutiérrez, J. Domínguez, P.A. Peixoto, Fernández, N. D. Rodríguez, D. Deffieux, L. Rojas, S. Quideau, L. Pouységu, J.E. Charris, Synthesis and leishmanicidal evaluation of sulfanyl and sulfonyl-tethered functionalized benzoate derivatives featuring a nitroimidazole moiety, Arch. Pharm. 353 (2020) e2000002, https://doi.org/10.1007/s00436-021-07266-w.
[26] J.E. Gutiérrez, E. Fernandez-Moreira, M.A. Rodríguez, M.R. Mijares, J.B. De Sanctis, Soňa S. Gurská, P. Džubák, M. Hajdůch, J. Bruno-Colmenarez, L. Rojas, D. Deffieux, L. Pouységu, S. Quideau, J. Charris, H. Ramírez, Novel 7-Chloro-(4-thioalkylquinoline) derivatives: synthesis and antiproliferative activity through inducing apoptosis and DNA/RNA damage, Pharmaceuticals 15 (2022) 1234, https://doi.org/10.3390/ph15101234.
[27] J.E. Gutiérrez, E. Fernandez-Moreira, M.E. Acosta, H. Ramírez, J.E. Charris, Optimization of the synthesis, in silico ADME/Tox profiling studies, and evaluation of the antimalarial activity of (7-chloroquinolin-4-ylthio) alkylbenzoate derivatives, J. Chem. Res. 47 (2023) 1–8, https://doi.org/10.1177/17475198231175326.
[28] H.-Q. Li, Z.-P. Xiao, R.-Q. Fang, H.-L. Zhu, The syntheses and crystal structures of metronidazole-derived compounds, J. Chem. Crystallogr. 38 (2008) 461–466, https://doi.org/10.1007/s10870-008-9343-9.
[29] B. Neises, W.S. Steglich, Simple method for the esterification of carboxylic acids, Angew. Chem. Int. Engl. 17 (1978) 522–524, https://doi.org/10.1002/anie.197805221.
[30] A. Daina, O. Michielin, V. Zoete, SwissADME: a free web tool to evaluate pharmacokinetics, drug-likeness and medicinal chemistry friendliness of small molecules, Sci. Rep. 7 (2017) 42717, https://doi.org/10.1038/srep42717.
[31] C.A. Lipinski, F. Lombardo, B.W. Dominy, P.J. Feeney, Experimental and computational approaches to estimate solubility and permeability in drug discovery and development settings, Adv. Drug Deliv. Rev. 46 (2001) 3–26, https://doi.org/10.1016/s0169-409x(00)00129-0.
[32] J.S. Delaney Esol, Estimating aqueous solubility directly from molecular structure, J. Chem. Inf. Comput. Sci. 44 (2004) 1000–1005, https://doi.org/10.1021/ci034243x.

[33] J. Ali, P. Camilleri, M.B. Brown, A.J. Hutt, S.B. Kirton, Revisiting the general solubility equation: in silico prediction of aqueous solubility incorporating the effect of topographical polar surface area, J. Chem. Inf. Model. 52 (2012) 420–428, https://doi.org/10.1021/ci200387c.
[34] D.E.V. Pires, T.L. Blundell, D.V. Ascher pkCSM, Predicting small-molecule pharmacokinetic and toxicity properties using graph-based signatures, J. Med. Chem. 58 (2015) 4066–4072, https://doi.org/10.1021/acs.jmedchem.5b00104.
[35] A. Daina, V. Zoete, A BOILED-Egg to predict gastrointestinal absorption and brain penetration of small molecules, ChemMedChem 11 (2016) 1117–1121, https://doi.org/10.1002/cmdc.201600182.
[36] R. Watanabe, T. Esaki, H. Kawashima, Y. Natsume-Kitatani, C. Nagao, R. Ohashi, K. Mizuguchi, Predicting fraction unbound in human plasma from chemical structure: improved accuracy in the low value ranges, Mol. Pharm. 15 (2018) 5302–5311, https://doi.org/10.1021/acs.molpharmaceut.8b00785.
[37] A. Daina, O. Michielin, V. Zoete, SwissTargetPrediction: updated data and new features for efficient prediction of protein targets of small molecules, Nucleic Acids Res. 47 (2019) W357–W364, https://doi.org/10.1093/nar/gkz382.
[38] A.K. Daly, A.E. Rettie, D.M. Fowler, J.O. Miners, Pharmacogenomics of CYP2C9: functional and clinical considerations, J. Pers. Med. 8 (2017) 1, https://doi.org/10.3390/jpm8010001.
[39] A.L. Del Tredici, A. Malhotra, M. Dedek, F. Espin, D. Roach, G.D. Zhu, J. Voland, T. A. Moreno, Frequency of CYP2D6 alleles including structural variants in the United States, Front. Pharmacol. 9 (2018) 305, https://doi.org/10.3389/fphar.2018.00305.
[40] K. Katsuno, J.N. Burrows, K. Ken Duncan, R.H. van Huijsduijnen, T. Kaneko, K. Kita, Hit and lead criteria in drug discovery for infectious diseases of the developing world, Nat. Rev. Drug Discov. 14 (2015) 751–758, https://doi.org/10.1038/nrd4683.
[41] P. Rohloff, A. Montalvetti, R. Docampo, Acidocalcisomes and the contractile vacuole complex are involved in osmoregulation in Trypanosoma cruzi, J. Biol. Chem. 279 (2004) 52270–52281, https://doi.org/10.1074/jbc.M410372200.
[42] B. Zingales, S.G. Andrade, M.R.S. Briones, D.A. Campbell, E. Chiari, O. Fernandes O, F. Guhl, E. Lages-Silva, A.M. Macedo, C.R. Machado, M.A. Miles, A.J. Romanha, N.R. Sturm, M. Tibayrenc, A.G. Schijman, A new consensus for *Trypanosoma cruzi* intraspecific nomenclature: second revision meeting recommends TcI to TcVI, Mem. Inst. Oswaldo Cruz 104 (2009) 1051–1054, https://doi.org/10.1590/S0074-02762009000700021.
[43] T. Mosmann, Rapid colorimetric assay for cellular growth and survival: application to proliferation and cytotoxicity assays, J. Immunol. Methods 65 (1983) 55–63, https://doi.org/10.1016/0022-1759(83)90303-4.
[44] A. Mijoba, E. Fernandez-Moreira, N. Parra-Giménez, S. Espinosa-Tapia, Z. Blanco, H. Ramírez, J. Charris, Synthesis of Benzocycloalkanone-based Michael acceptors and biological activities as antimalarial and antitrypanosomal agents, Molecules 28 (2023) 5569, https://doi.org/10.3390/molecules28145569.
[45] A.C. Schoijet, K. Miranda, W. Girard Dias, W. de Sousa, M.M. Flawiá, H.N. Torres, R. Docampo, G.D. Alonso, A *Trypanosoma cruzi* phosphatidylinositol 3-kinase (TcVps34) is involved in osmoregulation and receptor-mediated endocytosis, J. Biol. Chem. 283 (2008) 31541–31550, https://doi.org/10.1074/jbc.M801367200.